International Journal of Pharmaceutics 430 (2012) 238–246

Contents lists available at SciVerse ScienceDirect

International Journal of Pharmaceutics

journal homepage: www.elsevier.com/locate/ijpharm

Pharmaceutical Nanotechnology

Emodin loaded solid lipid nanoparticles: Preparation, characterization and antitumor activity studies

Shengpeng Wang[a,1], Tongkai Chen[b,1], Ruie Chen[a], Yangyang Hu[a], Meiwan Chen[a,*], Yitao Wang[a,*]

[a] State Key Laboratory of Quality Research in Chinese Medicine, Institute of Chinese Medical Sciences, University of Macau, Av. Padre Tomas Pereira S.J., Taipa, Macau, 999078, China
[b] Guangzhou Institute of Pharmaceutical Industry, Guangzhou, 510240, China

ARTICLE INFO

Article history:
Received 22 November 2011
Received in revised form 24 February 2012
Accepted 16 March 2012
Available online 23 March 2012

Keywords:
Emodin
Solid lipid nanoparticles
High pressure homogenization
Antitumor

ABSTRACT

The objective of the present study was to prepare and characterize emodin (EMO)-loaded solid lipid nanoparticles (E-SLNs) and evaluate their antitumor activity *in vitro*. EMO and pharmaceutical lipid material were used to prepare E-SLNs by high pressure homogenization (HPH). Poloxamer 188 and Tween 80 were used as surfactants. The physicochemical properties of the E-SLNs were investigated by particle size analysis, zeta potential measurement, drug entrapment efficiency (EE), stability and *in vitro* drug release behavior. The E-SLNs showed stable particle size at 28.6 ± 3.1 nm, ideal drug EE and relative long-term physical stability after being stored for 4 months. The drug release of E-SLNs could last 72 h and exhibited a sustained profile, which made it a promising vehicle for oral drug delivery. MTT assay showed that E-SLNs could significantly enhance the *in vitro* cytotoxicity against human breast cancer cell line MCF-7 and MDA-MB-231 cells compared to the EMO solution, while free EMO, blank SLNs (B-SLNs) and E-SLNs all showed no significant toxicity to human mammary epithelial line MCF-10A cells. Flow cytometric analysis demonstrated that E-SLNs also showed more significant cell cycle arrest effect in MCF-7 cells compared to bulk EMO solution. Hoechst 33342 staining and Annexin V-FITC/PI double staining further confirmed that E-SLNs induced higher apoptotic rates in MCF-7 cells, indicating that cell cycle arrest and apoptosis maybe the underlying mechanism of the enhanced cytotoxicity. Taken together, it seems that HPH was a simple, available and effective method for preparing high quality E-SLNs to enhance its aqueous solubility. Moreover, these results suggest that the delivery of EMO as lipid nanoparticles maybe a promising approach for cancer therapy.

1. Introduction

The pharmaceutical industry has long faced with the puzzle of fully utilization of many poor water-soluble drugs. Poor hydrophilicity has led to many regrettable failures in new drug development, which aroused many attempts to break the technical challenge. Solid lipid nanoparticles (SLNs) attract major attention as a new drug delivery system for anticancer drugs, peptides and proteins, and gene therapy (Almelda and Souto, 2007; del Pozo-Rodriguez et al., 2009; Wong et al., 2007). SLNs delivery systems possess plenty of advantages including controlled release, targeting purposes and prevention of the loaded drugs from degradation (Blasi et al., 2007; Ying et al., 2011). Moreover, SLNs play an important role in pharmaceutical applications due to the excellent physicochemical and biological properties with small diameter and narrow size distribution (Chattopadhyay et al., 2007). SLNs offer an attractive means for drug delivery, particularly for poorly water-soluble drugs.

Emodin (EMO, 3-methyl-1,6,8-trihydroxyanthraquinone, Fig. 1), a Chinese herbal anthraquinone derivative, can be isolated from many medicinal herbs such as Rhubarb (*Rheum officinale* B.), Aloe (*Aloe barbadensis* M.) and leaf of Senna (*Cassia angustifolia*) (Huang et al., 2007; Srinivas et al., 2007). EMO has attracted much attention in recent years because of its multiple biological activities, such as vasorelaxative, immunosuppressive, hepatoprotective and its anti-tumor activities (Pan et al., 2010; Srinivas et al., 2007). EMO is proven to be a promising anti-tumor agent which mechanism is associated with its capabilities of inhibiting proliferation, cell cycle arrest, induction of apoptosis and prevention of metastasis (Chen et al., 2010; Fu et al., 2007; Hsu et al., 2010). These capabilities are believed to act through NF-kappa B (NF-kB), phosphoinositol 3-kinase (PI3K), and mitogen-activated protein kinase (MAPK) signaling pathways (Huang et al., 2005; Ko et al., 2010; Wei et al., 2010).

In spite of the distinctive biological activities, it is well known that EMO presents a poor oral bioavailability due to its extremely low water solubility, which is shared by much of anthraquinone

* Corresponding authors. Tel.: +853 83974873; fax: +853 28841358.
E-mail addresses: mwchen@umac.mo (M. Chen), ytwang@umac.mo (Y. Wang).
[1] These authors contributed equally to this work.

0378-5173/$ – see front matter.
doi:10.1016/j.ijpharm.2012.03.027

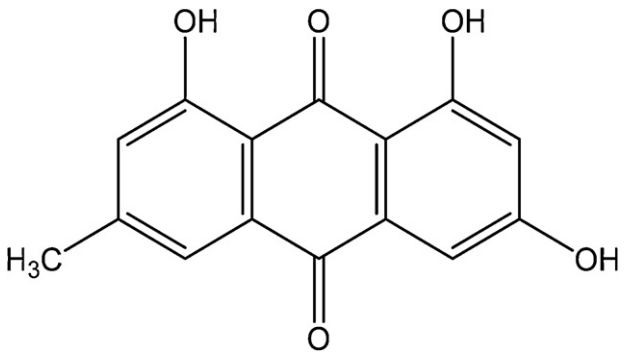

Fig. 1. Chemical structure of emodin.

compounds. Emodin is a naturally occurring anthraquinone which is widely used as a laxative and has other versatile biological activities. It is practically insoluble in water and soluble in alcohol, aqua alkali hydroxide solutions. Like a phenolic compound, emodin behaviors as an acid (in acetonitrile) pK_a: 5.70 and 7.94. Emodin is more acidity than phenol, pK_a of phenol is 9.89. This chemical property must be taken account when one investigates emodin in aqua solution. Moreover, emodin belongs to BCS classification II, which means low solubility but high permeability. The bioavailability of emodin is limited by its salvation rate. In the present study, we tried to prepare EMO loaded SLNs to enhance its anti-tumor activity. We assessed the feasibility of high pressure homogenization technique, and characterized the physicochemical properties of E-SLNs including particle size analysis, zeta potential measurement, drug entrapment efficiency, physical stability and *in vitro* drug release behavior, and evaluated its antitumor activity *in vitro*. We hypothesized that the anti-cancer activity of E-SLNs may be different from the free drug, thus the toxicity, the effect on cell cycle and cell apoptosis with breast cancer cells were further investigated. These results showed the promise of potential applications of delivering EMO as solid lipid nanoparticles for cancer therapy.

2. Materials and methods

2.1. Materials

EMO was purchased from Nanjing Zelang Medical Technology Co., LTD, and the purity was determined to be 98% by high-performance liquid chromatography. Glycerol monostearate (GMS), stearic acid and Tween 80 were all purchased from Guangzhou Chemical Reagent Factory (China). Poloxamer 188 (F68) was provided by Sigma (Aldrich Laborchemikalien GmbH). RPMI-1640 culture medium was obtained from Gibco. Fetal bovine serum (FBS), phosphate-buffered saline (PBS), penicillin–streptomycin (PS), 0.25% (w/v) trypsin/1 mM EDTA, Hoechst 33342 and Propidium iodide (PI) were purchased from Invitrogen. 3-[4,5-dimethyl-2-thiazolyl]-2,5-diphenyl tetrazolium bromide (MTT) were obtained from Molecular Probes. Annexin V-FITC/PI apoptosis detection kit was purchased from BD. Other chemicals were of analytical grade from local sources and used without further purification. All reagents were used as received.

2.2. High performance liquid chromatograph (HPLC) analysis of E-SLNs

The drug EMO was detected by high performance liquid chromatograph (HPLC) consisted of Dionex UltiMate 3000 Pump, an autosampler, a diode array detector (DAD detector), a Kromasil C_{18} (4.6 mm × 250 mm, 5 μm) analytical column and a workstation. The UV detector was operated at 254 nm. Mobile phase was methanol/0.1% phosphate solution (85:15), and flow rate was kept at 1.0 ml/min at ambient temperature. Aliquots of 20 μL clear supernatant samples were injected into the HPLC system. The detection limit of EMO was 0.5 ng/mL. Intra- and interday variabilities were below 1.5%. All the samples were filtered through an aqueous 0.45 μm pore size filter membrane in order to protect the column.

2.3. Preparation of E-SLNs

E-SLNs were prepared by high pressure homogenization (HPH). EMO and pharmaceutical lipid material were weighed precisely with electronic balance (Sartorius BS224S) and dissolved in water bath at 70–80 °C (10–15 °C above the melting point of the lipid). Surfactants were dissolved in breaker with water, and then added into melted EMO drop by drop over 70–80 °C water bath. The obtained pre-emulsion was passed through a high pressure homogenizer (NS1001L Niro Soavi S.P.A). The samples were stored in refrigerator at 4 °C.

2.4. Characterization of E-SLNs

2.4.1. Measurement of particle size and zeta potential for E-SLNs

In order to assess the feasibility of the preparation methods, particle size analysis were performed on the production day. Particle size and zeta potential of E-SLNs were measured by photon correlation spectroscopy using Malvern Zetasizer (3000HS. Malvern Instruments Ltd.). All the samples were diluted with aqueous phase of the formulation to get optimum kilo counts per second (kcps) of 50–200 for measurements.

2.4.2. Determination of drug entrapment efficiency

The entrapment efficiency (EE) was calculated from the ratio of the drug amount incorporated into the SLNs to the total charged drug amount. The EE of E-SLNs was directly determined by ultrafiltration method using centrifugal filter tubes with a 50,000 Da molecular weight cut-off. Briefly, 2 ml of E-SLNs dispersion was placed into a centrifugal filter tube which was centrifuged at 4000 rpm for about 15 min at room temperature. The SLN along with encapsulated drug remained in the outer chamber and dispersion medium moved to the sample recovery chamber through filter membrane. The amount of free drug in the aqueous phase after isolation of the system was detected by HPLC. The amount of incorporated drug was calculated by subtracting free drug from initial drug. The EE of E-SLNs was calculated according to the following equation (Luo et al., 2006; Souto et al., 2004):

$$\mathrm{EE} = \frac{W_{\text{initial drug}} - W_{\text{free drug}}}{W_{\text{initial drug}}} \times 100\% \quad (1)$$

where $W_{\text{initial drug}}$ is the amount of drug used for the assay and $W_{\text{free drug}}$ is the amount of free drug detected in the aqueous phase after isolation of the suspension.

2.4.3. Stability study

E-SLNs dispersion was stored at room temperature for 4 months under a sealed condition and evaluated by clarity, particle size and drug entrapment efficiency at 0th, 1st, 2nd, 3rd and 4th months after prepared. Each sample was detected for three times.

2.5. Evaluation of in vitro drug release

In vitro drug release was performed using the dialysis bag method. Phosphate buffer (PBS, pH 6.8) was used as dissolution medium. The dialysis bag (molecular weight cut off 8000–13,000 Da) could retain SLNs and allow the diffusion of free drug into dissolution medium. The bags were soaked in DI water for

24 h before being used. 1 ml of E-SLNs dispersion was poured into the bag with the two ends fixed by strings. The bags were placed in a conical flask and 10 ml dissolution medium was added. The conical flasks were placed into a thermostatic shaker (THZ-8Z; Jiangsu Jintan Honghua Instrument Factory, Jiangsu, China) at 37 °C with a rate of 100 rpm. At 0.5, 1, 2, 3, 4, 6, 8, 10, 12, 24, 36, 48, 72 h after test, the medium in the conical flask was removed for analysis and fresh dialysis medium was then added to maintain sink conditions. The drug contents in samples were analyzed by the HPLC method. All the operations were carried out in triplicate.

2.6. Cell culture study

The MCF-7 (0.8×10^4), MDA-MB-231 (1.0×10^4) and MCF-10A (1×10^4) cells were obtained from the American Type Culture Collection (ATCC). Cells were cultured in RPMI-1640 medium with antibiotics (100 U/ml penicillin and100 μg/ml streptomycin) and 10% (v/v) heat-inactivated FBS at 37 °C under 5% CO_2.

2.6.1. MTT assay

The cell viability was estimated by MTT assay as described previously (Zhong et al., 2011). MCF-7 (0.8×10^4), MDA-MB-231 (1.0×10^4) and MCF-10A (1×10^4) cells were seeded into a 96-well plate and allowed to attach for 24 h. When reaching approximately 70–80% confluence, the cells were incubated with a serum-free medium for 24 h, then the cells were treated with different concentrations of free EMO and E-SLNs for 12, 24 and 48 h, respectively. After treatment, cell viability was determined by being incubated with medium containing MTT (1 mg/ml) for 4 h, followed by dissolving the formazan crystals with DMSO. The absorbance at 570 nm was determined with a microplate reader and presented as relative cell viability. Percent of cell survival was defined as the relative absorbance of treated cells *vs.* respective controls.

2.6.2. Cell cycle analysis

Cell cycle distribution based on the DNA contents were determined as previously described (Gao et al., 2009). MCF-7 cells were seeded at the density of 1.0×10^6 cells in 25 ml Nunc cell culture flask and allowed to attach for 24 h. After starving for 24 h, cells were exposed to various concentrations of free EMO and E-SLNs for another 24 h. After washing twice with PBS, cells were harvested and collected by centrifugation at 300 g for 5 min, followed by fixing in ice-cold 70% ethanol under −20 °C overnight. Then, cells were collected by centrifugation and stained with 100 μl of PI stain solution (20 μg/ml PI, 8 μg/ml RNase) for 30 min (protected from light), followed by analyzing with a flow cytometer (BD FACS CantoTM, BD Biosciences, San Jose, USA). The cell distribution in phases of SubG1, G0/G1, S, and G2/M were measured and results were calculated by the ModFit LT software (version 3.0).

2.6.3. Hoechst 33342 staining

Apoptotic nuclear morphology was assessed by Hoechst 33342 staining (Li et al., 2011). MCF-7 cells were seeded in 24-well plates at a density of 3.0×10^5 per well. After 24 h of incubation, cells were treated with B-SLN, free EMO (20, 30 μM) and E-SLN (20, 30 μM). After 48 h treatment, cells were fixed with 4% paraformaldelyde for 30 min at room temperature, then washed by PBS and stained with 167 mM of Hoechst 33342 at room temperature for 30 min. Apoptotic nuclear morphology was observed with a fluorescent microscope (Olympus, Tokyo, Japan).

2.6.4. Apoptotic cell determination by Annexin V/PI staining assay

The Annexin V-FITC/PI apoptosis detection kit (BD, USA) was used to detect apoptotic cells. MCF-7 cells were exposed to different concentrations of EMO solution and E-SLN for 48 h. After 48 h incubation, cells were trypsinized and collected by centrifugation, then washed twice with PBS and gently resuspended in 100 μl binding buffer. Then 5 μl of Annexin-FITC and 10 μl of PI solution were added, after incubation in the dark at room temperature for 15 min according to manufacturer's instruction, cell apoptosis was analyzed with a flow cytometer (BD FACS CantoTM, BD Biosciences, San Jose, USA). Annexin V^+ and PI^- cells were scored as early apoptotic, and double-stained cells were considered as late apoptotic.

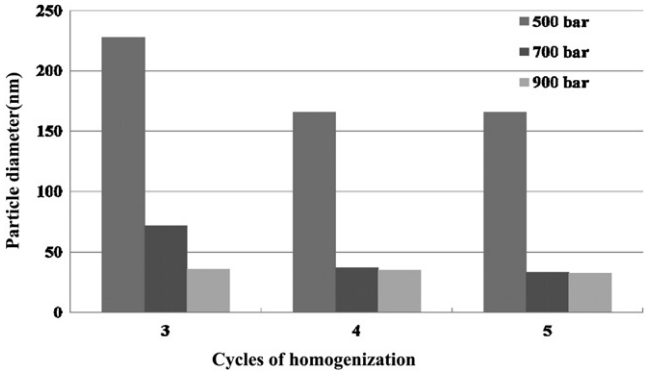

Fig. 2. Particle size of E-SLNs at different pressure with different cycles of homogenization.

2.7. Statistical analysis

The results were presented as Mean ± S.E. Statistical analysis was performed using Student's *t*-test with $p < 0.05$ indicating significant difference.

3. Results and discussion

3.1. Preparation of E-SLNs

3.1.1. Effect of different lipid material

In order to select a suitable lipid for E-SLNs, Compritol 888 ATO, glycerol monostearate (GMS), stearic acid and lauric acid were respectively used as the lipid materials of SLNs. We found that all the lipids could result in translucent dispersion. However, Compritol 888 ATO-based SLNs had a large particle size, lauric acid-based SLNs and GMS-based SLNs had a wide size distribution. All showed poor stability due to a large particle size and wide size distribution. While the stearic acid-based SLNs showed a suitable particle size and physical stability. Thus, stearic acid was selected as the optimum lipid for E-SLNs.

In addition, the pressure and cycle times of HPH were also investigated. The particle size of E-SLNs at 500, 700, 900 bar with 3, 4 and 5 cycles of homogenization were shown in Fig. 2. E-SLNs homogenized at 500 bar showed a relatively large particle size and also consistency of particle diameter with the increase of homogenization cycles. The pressure of 900 bar resulted in low particle size, but there was a slight decrease of particle size of E-SLNs with the increase of the homogenization cycles. The high pressure of homogenization might result in the formation of the small particles and then the small particles could aggregate to form large nanoparticles due to the absence of sufficient surfactants. E-SLNs homogenized at 700 bar with typically four homogenization cycles showed a narrow distribution and small diameters and then was selected as the optimum condition for preparation of the E-SLNs formulation.

3.1.2. Effect of lipid concentration

E-SLNs were prepared using stearic acid concentration of 15, 25 and 35 mg/mL at the aqueous phase. The mean particle diameter and EE of E-SLNs were shown in Fig. 3. We found that the lipid solution with the concentration above 65 mg/mL was unstable and

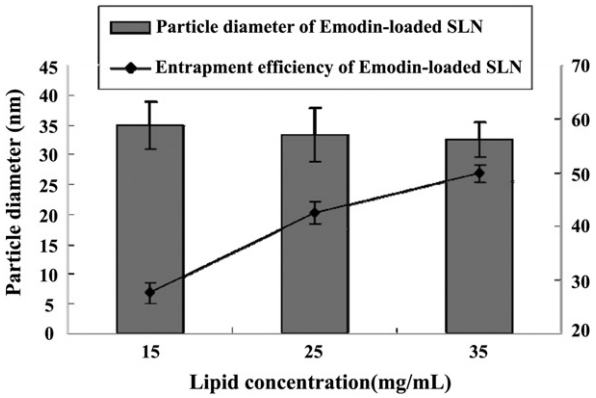

Fig. 3. Effect of lipid on the mean particle diameter and entrapment efficiency of E-SLNs prepared with concentration of 15, 25 and 35 mg/mL.

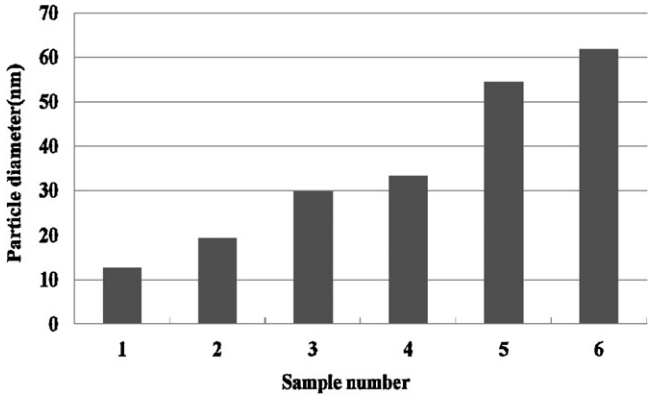

Fig. 4. The mean particle size of E-SLNs and sample numbers correspond with numbers listed in Table 1.

thus not used in this work. In the tested parameter range, the mean diameter of SLNs decreased slightly with an increase in the lipid concentration. But the concentration of lipid showed a significant effect on EE. The possible reason is that the increase in stearic acid concentration can afford more space to encapsulate drug under the condition of given surfactant mixture in outer phase. Therefore, it was obvious that the suitable concentration of lipid was 35 mg/mL in the SLNs formulation.

3.1.3. *Effect of ratios of drug to lipid*

The results of EE with different ratios of drug to lipid were showed in Table 1. It was evident that EE were strongly linked to the ratios of drug to lipid, the EE was improved as increase of these ratios until to the maximum value, and then dropped down. No matter that the weight of drug was heavier or lighter than this critical value; the EE could all be reduced more or less. In other words, the least amount of free drug was detected in the lipid suspensions of the highest EE sample, and *vice versa.* The lower EE meant the large amount of free drug was left in the aqueous solution of solid lipid suspensions. Along with the improvement of ratios of drug to lipid, the decrease of the EE might be attributed to some amount of lipid that could encapsulate certain amount of drug in SLN. Therefore, it was obvious that the favorable amount of drug encapsulated in 1 g lipid was about 30 mg in the SLN formulation while the lipid remained unchanged in type and weight.

Samples prepared by various ratios of drug to lipid displayed different mean particle size. From the data in Fig. 4, it was clear that the average particle size increased with the increasing amount of drug when the lipid weights were unchanged. Additional, it was found that the lowest zeta potential took place at the sample with the highest EE.

It seemed that the interaction between the drug and the lipid during the preparation in that drug could influence some properties of the nanodispersion system, such as the mean particle size and EE. And drug was also altered by the nanometer carriers for the great increase of amorphous degree.

Table 1
Effect of ratios of drug to lipid (D:L) on the EE.

No.	D:L (w/w)	EE (%)
1	0.010:1	28.78
2	0.020:1	33.42
3	0.030:1	52.53
4	0.040:1	46.77
5	0.060:1	38.91
6	0.080:1	26.37

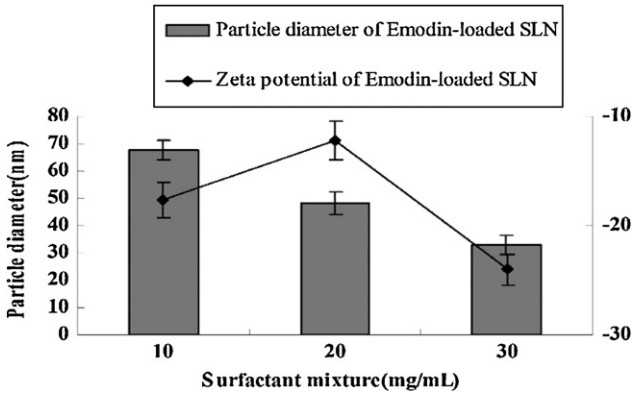

Fig. 5. Effect of total amount of surfactant mixture on the mean particle diameter and zeta potential of E-SLNs. SLN was prepared with 10, 20, 30 mg/mL surfactant mixture composed of Poloxamer 188 and Tween 80 (1:1, w/w).

3.1.4. *Effect of amount of surfactant mixture*

The composition of the aqueous SLNs colloidal dispersion with regard to the surfactants proved it was very important with respect to the influence on particle size from the production process, the physical long-term stability during storage and drug release profiles. Therefore, Poloxamer 188 and Tween 80 were chosen as the test surfactants in outer phase to investigate whether the increase in the surfactant amount influenced the mean particle diameter of E-SLNs.

As expected, the mean particle diameter of E-SLNs tended to decrease with increase in the total amount of surfactant mixture from 10 to 30 mg/mL (Fig. 5). The mean particle diameter could

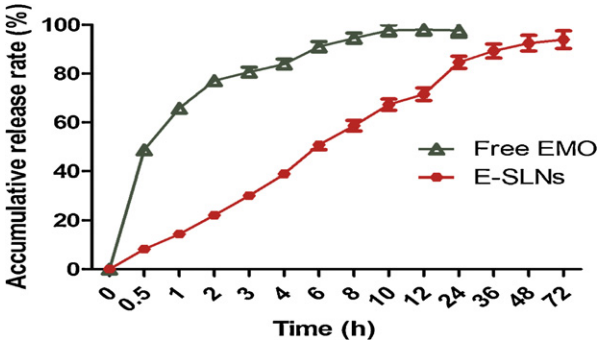

Fig. 6. Drug release profiles of E-SLNs *in vitro*.

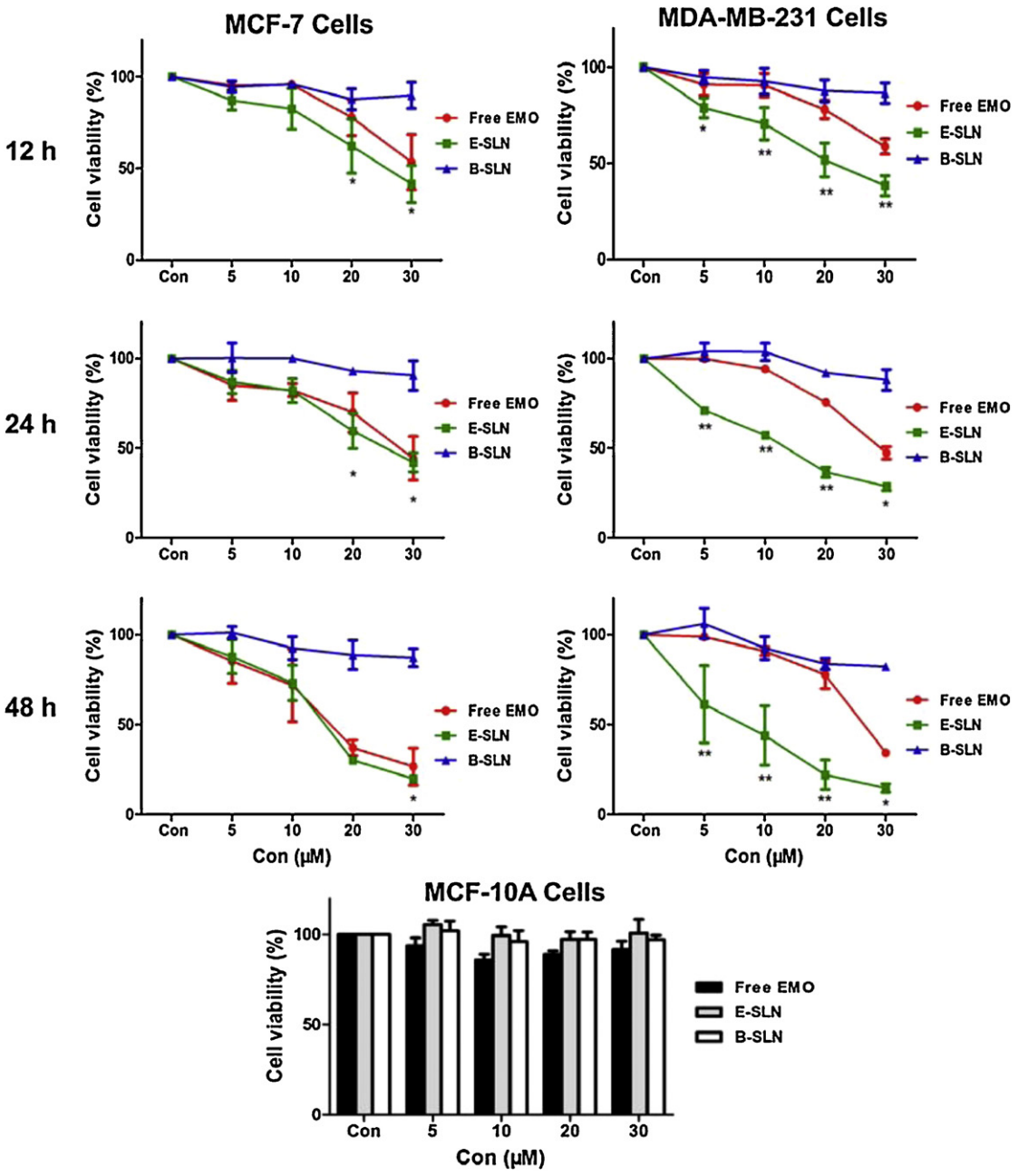

Fig. 7. MTT assay showing that both E-SLNs and free EVO solution (0–100 μM) treatment could inhibit growth of MCF-7 cells in a time- and dose-dependent manner. While B-SLNs showed negligible effect on cell viability and all of the three formations showed no significant toxicity to human nomal mammary epithelial cells. Results are expressed as mean ± standard deviation ($n = 3$). * $p < 0.05$ *vs.* the same concentration of free EMO solution group.

be reduced to 33.3 ± 3.4 nm by preparation SLN with 30 mg/mL surfactant mixture, while that of SLN with 10 mg/mL surfactant mixture was 67.8 ± 3.5 nm. The results might be related to the effects of the hydrophile-lipophile balance (HLB) value and the structure of the surfactants. Moreover, the EE was affected by the concentration of the surfactant mixture in outer phase. That is largely due to the high concentration of Poloxamer 188 and Tween 80, which caused the increasing thickness of the hydrophlic coating, and then more drugs can disperse and dissolve in it.

The change of total amount of surfactant mixture did not significantly affect the zeta potential of SLN (−17 to −24 mV) (Fig. 5). From these results, we fixed the total amount of surfactant mixture as 30 mg/mL.

3.2. The characterization of optimized E-SLNs

The mean particle size and zeta potential of colloidal carriers are important characteristics of SLN from which the stability of drug-loaded SLN can be predicted. The mean diameter and zeta potential of the optimized E-SLNs were 28.6 ± 3.1 nm, −31 ± 1.1 mV, respectively. The formulation consisting of certain amount of the above surfactant mixture was studied for the first time with the smallest mean particle size. The EE was 60.37 ± 2.2%.

3.3. Drug release profiles of E-SLNs

The E-SLNs were comprised of a high melting point stearic acid core with a protective coating of Poloxamer 188 and Tween

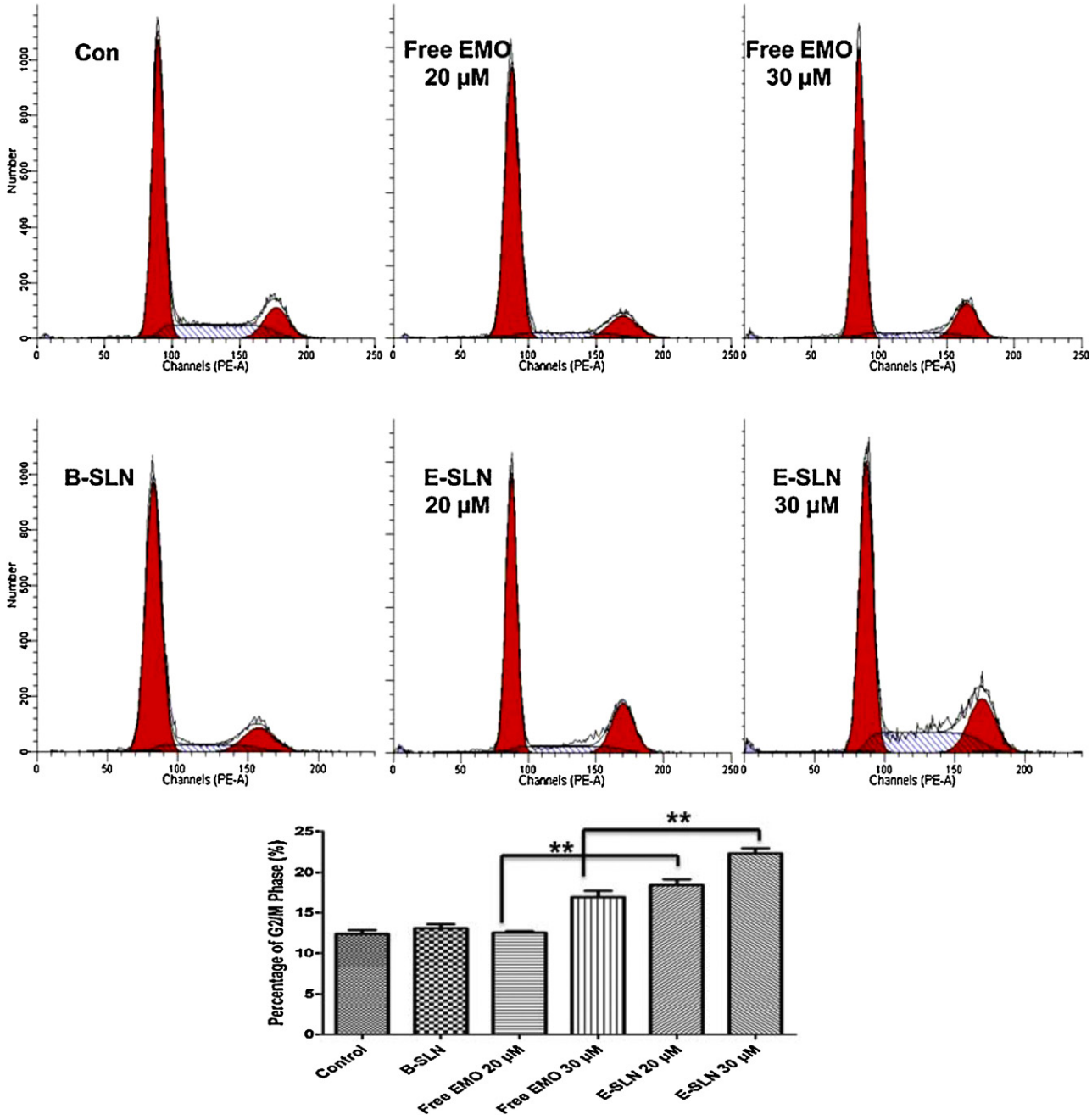

Fig. 8. Effect of E-SLNs, B-SLN and free EVO solution (0, 20, 30 μM) on the cell cycle distribution of MCF-7 cells. The various phases of the cell cycle were evaluated by flow cytometry. E-SLNs and free EVO solution induced MCF-7 cell cycle arrest at the G2/M in a dose-dependent manner, while B-SLN showed no effect on cell cycle distribution. Con, control. Data were expressed as mean ± S.E. * $p < 0.05$ *vs.* Control, ** $p < 0.01$ *vs.* Control.

80. The drug incorporation model relates to specific nature of the solid lipid matrix and the lipophilicity of drug. Only the drug with moderate lipophilicity can be loaded at high rate.

The drug release exhibited a biphasic pattern, burst drug release and sustained drug release. The release profile of E-SLNs resembled the drug-enriched core model (Fig. 6). The burst release of SLNs formulation at the initial period may be produced by the unencapsulated drug and absorption of drug on the surface of SLNs. Under the experimental conditions, E-SLNs possessed a sustained drug release over a period of 72 h. From Fig. 6 in the paper, we know that the *in vitro* drug release in 24 h was about 80%, and the later release lasted to 72 h, which matched with the physiological requirement for human. For oral application, both burst drug release and sustained drug release are of importance. Burst release can be useful for improving the penetration of drug, while sustained release will be beneficial for drug with irritation effect at high concentration.

Table 2
The IC_{50} values (μmol/L) of EMO and E-SLN on breast cancer cells.

Cells	Formation	12 h	24 h	48 h
MCF-7	Free EMO	31.73	29.62	15.79
	E-SLN	25.64	25.18	14.63
MDA-MB-231	Free EMO	39.66	29.07	26.05
	E-SLN	20.40	12.06	7.88

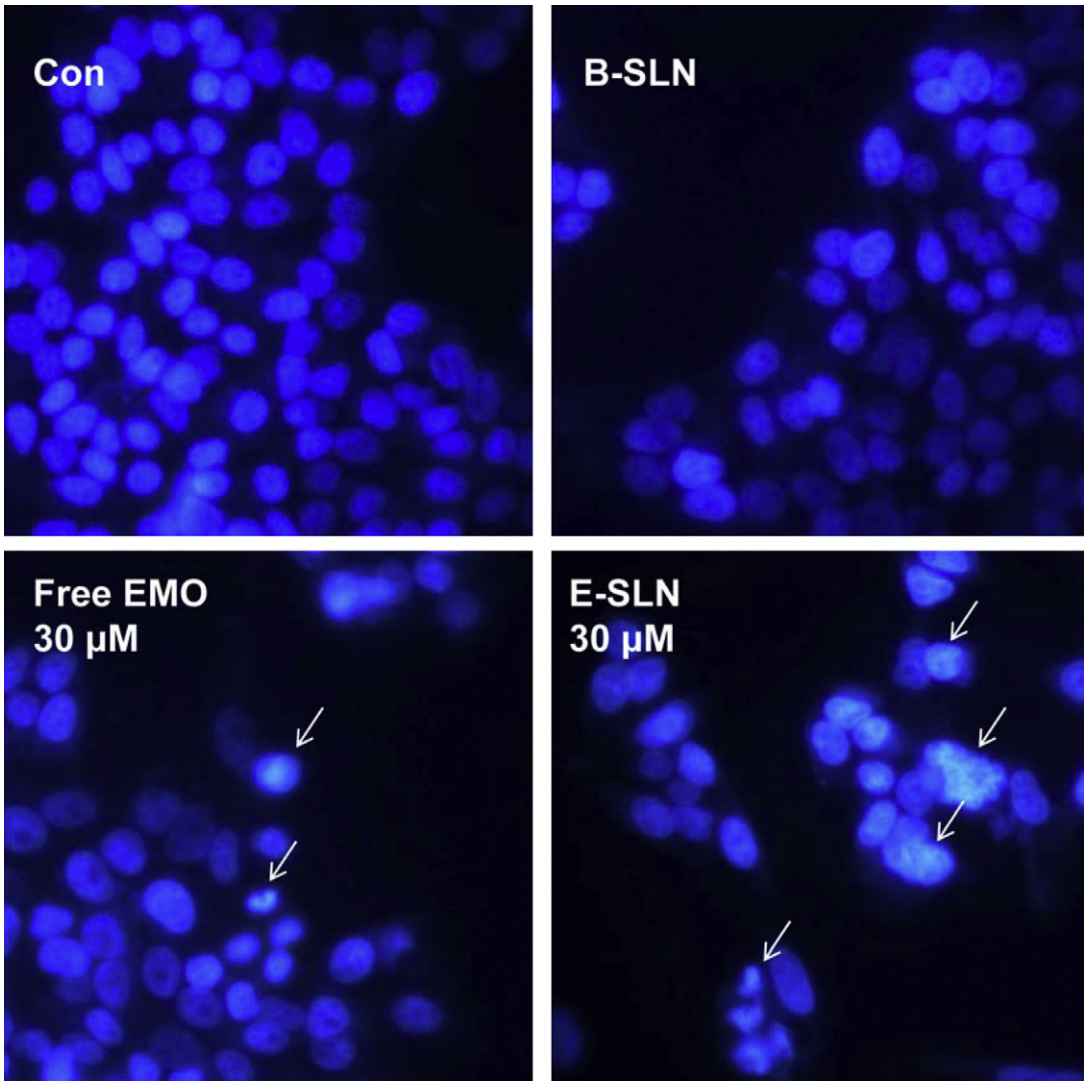

Fig. 9. Hoechst 33342 fluorescent staining to detect apoptotic morphology in breast cancer cells. MCF-7 cells were treated with B-SLN, free EMO (20, 30 μM) and E-SLN (20, 30 μM) for 48 h. Cells were observed using a fluorescent microscope (Olympus, Tokyo, Japan).

3.4. Stability study of optimized E-SLNs

E-SLNs dispersion was stored at room temperature for 4 months under a sealed condition and evaluated by clarity, particle size and drug entrapment efficiency after prepared. Each sample was detected for three times.

3.5. In vitro anticancer activity assay

3.5.1. In vitro cytotoxicity of free EMO and E-SLNs against breast cancer cells

The cellular cytotoxicity assays of free EMO, B-SLNs and E-SLNs were carried out on MCF-7, MDA-MB-231 breast cancer cells and human mammary epithelial cell line MCF-10A cells. MTT assay showed that both free EMO and E-SLNs could significantly suppressed MCF-7 cell proliferation in a dose- and time-dependent manner. While at the same concentration, E-SLNs showed significantly higher inhibition rates against both MCF-7 and MDA-MB-231 cells compared to free EMO solution (Fig. 7). The dose required for 50% growth inhibition (IC_{50} value) for free EMO and E-SLNs was calculated and shown in Table 2. Our study showed that the IC_{50} values of E-SLNs were much lower than that of free EMO at each time point. Meanwhile, in all toxicity study, B-SLNs were taken as respective controls for free EMO and E-SLNs. We found that B-SLNs showed negligible effect on cell viability (Fig. 7), thus the cytotoxicity effect of E-SLNs was confirmed to be because of EMO. Furthermore, in order to investigate the toxicity to normal cells, we also tested the toxicity of free EMO, B-SLNs and E-SLNs to MCF-10A cells. All of the three formations showed no significant toxicity to human normal mammary epithelial cells, which further confirmed the safety to normal cells.

Confusingly, in our study, the *in vitro* drug release study showed that free EMO released more than E-SLN within 24 h, but the MTT results showed that E-SLNs possessed stronger anti-tumor activity in both MCF-7 and MDA-MB-231 cells than free EMO within 24 h. This sounds and seems contradictory but is reality. Numerous researches have shown that nanoparticulate drug delivery systems can enhance antitumor activities of many chemotherapeutic drugs. When SLNs are close to the cell membrane, several physiological effects may occur at the same time. Nanoparticles can be internalized into cells *via* endocytosis or phagocytosis or just adsorbed on the surface of the cells (Mulik, 2010 #52) (des Rieux, 2006 #53). Though EMO was slowly released from E-SLNs, that does not mean, however, that the anti-tumor effect of E-SLN was postponed. The possible reason can be interpreted as follows. First, though free EMO had a relative burst drug release at the initial stage, the

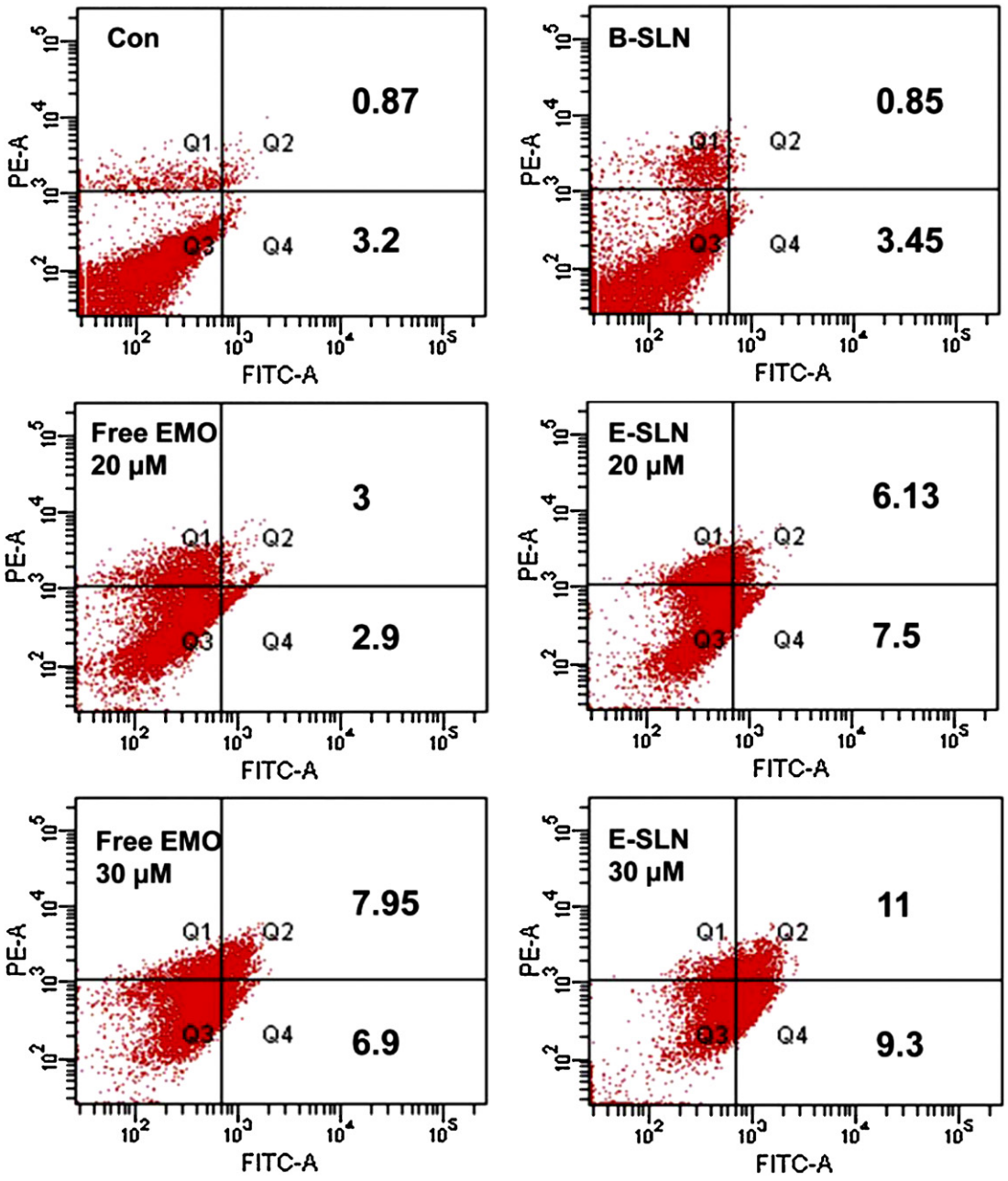

Fig. 10. Quantitative apoptotic measurement in MCF-7 cells after treatment with B-SLN, free EMO (20, 30 μM) and E-SLN (20, 30 μM) for 48 h. Top left (Q1): necrotic cells. (Annexin V-FITC$^-$PI$^+$); top right (Q2): late apoptotic cells (AnnexinV-FITC$^+$PI$^+$); bottom left (Q3): live cells (Annexin V-FITC$^-$PI$^-$); bottom right (Q4): early apoptotic cells (Annexin V-FITC$^+$PI$^-$).

drug was not efficaciously uptaked by cells. While for SLNs, the cellular uptake could be accelerated, because SLNs can be non-specifically internalized into cells *via* endocytosis or phagocytosis. Second, When SLNs attached to the cell membrane, the interactions between nanoparticles and cell membranes can affect the structure and properties of lipid bilayers as well as functions of those biomacromolecules on the biomembrane, such as ion channels, *etc.* Therefore, the attachment of SLNs to cell membrane is not as simple as physical adsorption, the homeostasis of cells can be consequently altered, which further contributed to the cytotoxicity of SLNs. Third, E-SLNs, possessing a markedly increased solubility and dissolution rate, could induce higher molecular concentration around the cells. The increased anti-tumor effect may also be associated with the more efficient uptake of tumor cells to drug delivered as SLNs.

3.5.2. Cell cycle analysis

EMO has already been shown to influence cell cycle distribution in various kinds of cells (Chun-Guang et al., 2010; Hsu et al., 2010; Kwak et al., 2006). Fig. 8 shows the cell cycle histograms of MCF-7 cells treated with E-SLNs and EMO solution at different concentration (0, 20, 30 μM) for 24 h. The flow cytometry assay showed that E-SLNs and EMO solution could arrest MCF-7 cells specifically at G2/M phase cell cycle in a dose-dependent manner. Following exposure to EMO solution and E-SLNs at 20 μM for 24 h, the percentage of cells in G2/M phase were 12.55% and 22.34%, respectively, both higher than that of the control group (12.37%). When the concentration increased to 30 μM, the fraction of cells in G2/M phase rose to 18.43% and 23.33%, respectively. These data suggested that E-SLNs showed more significant cell cycle arrest effect at G2/M

phase in MCF-7 cells compared to free EMO solution at the same concentration.

3.5.3. Cell apoptosis analysis

The deregulation of cell cycle has been proved to correlate with the induction of apoptosis. It was previously reported that EMO can induce apoptosis in human breast cancer cells (Huang et al., 2008). Based on the cell cycle analysis, we further characterized the EMO/E-SLN-induced apoptosis by Hoechst 33342 staining and Annexin V/PI dual staining. As shown in Fig. 9, cell nucleis were round and homogeneously stained in control and B-SLN group, however, EMO (30 μM)-treated MCF-7 cells showed marked nuclei blebbling and apoptotic bodies. The morphological changes of cell nucleis were more obvious in E-SLN group, indicating that the apoptotic effects were enhanced.

Annexin V/PI double staining is a more sensitive method in detecting apoptosis. Externalization of phosphatidyl serine (PS) from the inner side to outer leaflet of the cell membrane is an important indication of early apoptosis. Annexin V possesses a high affinity towards PS, early apoptotic cells can be easily detected by fluorescently labeled Annexin V. Meanwhile, PI can detect necrotic cells due to its permeability through the damaged cell membranes (Lou et al., 2011). As shown in Fig. 10, after 48 h treatment, both free EMO and E-SLN induced MCF-7 cell apoptosis in a dose-dependent manner. The percentage of Annexin V-staining cells (Q2 and Q4) was 5.9% and 14.85% for free EMO at 20 μM and 30 μM, respectively. While for E-SLNs at 20 μM and 30 μM, the percentages were 13.63% and 20.3%, respectively. Obviously, in comparison with free EMO, E-SLNs could promote a higher apoptotic rate in MCF-7 cells at the same dose. Our results were consistent with the previous studies, and also agreed with that of our *in vitro* cytotoxicity experiments.

4. Conclusions

In the present study, E-SLNs were prepared by high pressure homogenization technique. The method resulted in consistent production of smaller size solid lipid nanoparticles with narrow size distribution and good entrapment efficiency. The surfactant (Poloxamer 188 and Tween 80) concentration was optimized at 30 mg/mL based on the particle size and zeta potential. The *in vitro* release profile and stability data indicated sustained release of the drug and excellent physical long-term stability. The cellular cytotoxicity tests using MCF-7 cells demonstrated that E-SLNs were more cytotoxic than free EMO solution. Flow cytometry analysis further indicated that E-SLNs could arrest MCF-7 cells at G2/M phase more significantly compared to bulk EMO solution. Apoptosis studies also confirmed that E-SLNs induced higher apoptotic rates in MCF-7 cells, indicating that cell cycle arrest and apoptosis maybe the underlying mechanism of the enhanced cytotoxicity. Based on these results, we can conclude that the E-SLNs developed in this work may be a promising drug delivery strategy, especially for relatively insoluble anticancer drugs.

Acknowledgment

This study was supported by the Research Fund of the University of Macau (MYRG 208 (Y2-L4)-ICMS11-WYT and UL016/09-Y4/CMS/WYT01/ICMS).

References

Almelda, A.J., Souto, E., 2007. Solid lipid nanoparticles as a drug delivery system for peptides and proteins. Adv. Drug Deliv. Rev. 59, 478–490.
Blasi, P., Glovagnoli, S., Schoubben, A., Ricci, M., Rossi, C., 2007. Solid lipid nanoparticles for targeted brain drug delivery. Adv. Drug Deliv. Rev. 59, 454–477.
Chattopadhyay, P., Shekunov, B.Y., Yim, D., Cipolla, D., Boyd, B., Farr, S., 2007. Production of solid lipid nanoparticle suspensions using supercritical fluid extraction of emulsions (SFEE) for pulmonary delivery using the AERx system. Adv. Drug Deliv. Rev. 59, 444–453.
Chen, Y.Y., Chiang, S.Y., Lin, J.G., Ma, Y.S., Liao, C.L., Weng, S.W., Lai, T.Y., Chung, J.G., 2010. Emodin, aloe-emodin and rhein inhibit migration and invasion in human tongue cancer SCC-4 cells through the inhibition of gene expression of matrix metalloproteinase-9. Int. J. Oncol. 36, 1113–1120.
Chun-Guang, W., Jun-Qing, Y., Bei-Zhong, L., Dan-Ting, J., Chong, W., Liang, Z., Dan, Z., Yan, W., 2010. Anti-tumor activity of emodin against human chronic myelocytic leukemia K562 cell lines in vitro and in vivo. Eur. J. Pharmacol. 627, 33–41.
del Pozo-Rodriguez, A., Solinis, M.A., Gascon, A.R., Pedraz, J.L., 2009. Short- and long-term stability study of lyophilized solid lipid nanoparticles for gene therapy. Eur. J. Pharm. Biopharm. 71, 181–189.
Fu, Z.Y., Han, J.X., Huang, H.Y., 2007. Effects of emodin on gene expression profile in small cell lung cancer NCI-H446 cells. Chin. Med. J. (Engl.) 120, 1710–1715.
Gao, J.L., He, T.C., Li, Y.B., Wang, Y.T., 2009. A traditional Chinese medicine formulation consisting of *Rhizoma Corydalis* and *Rhizoma Curcumae* exerts synergistic anti-tumor activity. Oncol. Rep. 22, 1077–1083.
Hsu, C.M., Hsu, Y.A., Tsai, Y., Shieh, F.K., Huang, S.H., Wan, L., Tsai, F.J., 2010. Emodin inhibits the growth of hepatoma cells: finding the common anti-cancer pathway using Huh7, Hep3B, and HepG2 cells. Biochem. Biophys. Res. Commun. 392, 473–478.
Huang, Q., Shen, H.M., Ong, C.N., 2005. Emodin inhibits tumor cell migration through suppression of the phosphatidylinositol 3-kinase-Cdc42/Rac1 pathway. Cell. Mol. Life Sci. 62, 1167–1175.
Huang, Q., Lu, G., Shen, H.M., Chung, M.C., Ong, C.N., 2007. Anti-cancer properties of anthraquinones from rhubarb. Med. Res. Rev. 27, 609–630.
Huang, Z., Chen, G., Shi, P., 2008. Emodin-induced apoptosis in human breast cancer BCap-37 cells through the mitochondrial signaling pathway. Arch. Pharm. Res. 31, 742–748.
Ko, J.C., Su, Y.J., Lin, S.T., Jhan, J.Y., Ciou, S.C., Cheng, C.M., Lin, Y.W., 2010. Suppression of ERCC1 and Rad51 expression through ERK1/2 inactivation is essential in emodin-mediated cytotoxicity in human non-small cell lung cancer cells. Biochem. Pharmacol. 79, 655–664.
Kwak, H.J., Park, M.J., Park, C.M., Moon, S.I., Yoo, D.H., Lee, H.C., Lee, S.H., Kim, M.S., Lee, H.W., Shin, W.S., Park, I.C., Rhee, C.H., Hong, S.I., 2006. Emodin inhibits vascular endothelial growth factor-A-induced angiogenesis by blocking receptor-2 (KDR/Flk-1) phosphorylation. Int. J. Cancer 118, 2711–2720.
Li, Y.B., Lin, Z.Q., Zhang, Z.J., Wang, M.W., Zhang, H., Zhang, Q.W., Lee, S.M., Wang, Y.T., Hoi, P.M., 2011. Protective, antioxidative and antiapoptotic effects of 2-methoxy-6-acetyl-7-methyljuglone from *Polygonum cuspidatum* in PC12 cells. Planta Med. 77, 354–361.
Lou, H., Gao, L., Wei, X., Zhang, Z., Zheng, D., Zhang, D., Zhang, X., Li, Y., Zhang, Q., 2011. Oridonin nanosuspension enhances anti-tumor efficacy in SMMC-7721 cells and H22 tumor bearing mice. Colloids Surf. B Biointerf. 87, 319–325.
Pan, C.J., Wang, J., Huang, N., 2010. Preparation, characterization and in vitro anticoagulation of emodin-eluting controlled biodegradable stent coatings. Colloids Surf. B Biointerf. 77, 155–160.
Srinivas, G., Babykutty, S., Sathiadevan, P.P., Srinivas, P., 2007. Molecular mechanism of emodin action: transition from laxative ingredient to an antitumor agent. Med. Res. Rev. 27, 591–608.
Wei, W.I., Chen, H., Ni, Z.L., Liu, H.I., Tong, H.F., Fan, L., Liu, A., Qiu, M.U., Liu, D.L., Guo, H.C., Wang, Z.H., Lin, S.Z., 2010. Antitumor and apoptosis-promoting properties of emodin, an anthraquinone derivative from *Rheum officinale* Baill, against pancreatic cancer in mice via inhibition of Akt activation. Int. J. Oncol. 39, 1381–1390.
Wong, H.L., Bendayan, R., Rauth, A.M., Li, Y.Q., Wu, X.Y., 2007. Chemotherapy with anticancer drugs encapsulated in solid lipid nanoparticles. Adv. Drug Deliv. Rev. 59, 491–504.
Ying, X.Y., Cui, D., Yu, L.A., Du, Y.Z., 2011. Solid lipid nanoparticles modified with chitosan oligosaccharides for the controlled release of doxorubicin. Carbohydr. Polym. 84, 1357–1364.
Zhong, Z., Chen, X., Tan, W., Xu, Z., Zhou, K., Wu, T., Cui, L., Wang, Y., 2011. Germacrone inhibits the proliferation of breast cancer cell lines by inducing cell cycle arrest and promoting apoptosis. Eur. J. Pharmacol. 667, 50–55.